# A Three-Dimensional Multistep Horizontally Wide-Angle Beam-Propagation Method Based on the Generalized Douglas Scheme

# A Three-Dimensional Multistep Horizontally Wide-Angle Beam-Propagation Method Based on the Generalized Douglas Scheme

Jun Shibayama, *Member, IEEE*, Tatsuya Takahashi, Junji Yamauchi, *Member, IEEE*, and Hisamatsu Nakano, *Fellow, IEEE*

***Abstract*—A three-dimensional horizontally wide-angle beam-propagation method is formulated on the basis of the multistep method for higher order Padé approximants, together with the alternating-direction implicit scheme. The fourth-order accurate finite-difference formula is used to enhance the efficiency of the method. The effectiveness is demonstrated through the analyses of a tilted step-index waveguide and a multimode interference coupler.**

***Index Terms*—Alternating-direction implicit (ADI) scheme, beam-propagation method (BPM), multimode interference (MMI) coupler, multistep method, optical waveguide, Padé approximant.**

## I. Introduction

THE wide-angle beam-propagation method (WA-BPM) based on the Padé approximant [1]–[3] has widely been utilized to analyze various optical waveguides. The higher order Padé approximants are efficiently treated with the multistep method [4]. To improve the accuracy of the WA-BPM, highly accurate finite-difference (FD) formulas have often been used. For graded-index waveguides, we applied the generalized Douglas (GD) scheme to the WA-BPM with the multistep method, leading to the fourth-order accuracy in space [5], [6]. Chiou *et al.* extended the GD scheme to the analysis of step-index waveguides [7]. Although this GD-based improved-FD formula (IFD4) achieves the fourth-order accuracy, its application was limited to the modal analysis. Recently, we introduced the IFD4 into the WA-BPM with the (1,1) Padé approximant for the analysis of a waveguide-based demultiplexer [8]. Subsequently, Zhang *et al.* improved the IFD4-based WA-BPM using the multistep method [9]. Note, however, that all the WA-BPMs with the IFD4 were formulated only for two-dimensional (2-D) problems, although the Fresnel-based BPM with the IFD4 was developed for three-dimensional (3-D) problems [10].

For 3-D problems, the noniterative alternating-direction implicit (ADI) scheme was not applied to the wide-angle formulation [11], [12], since the direct application gives rise to the zeroth-order splitting error term. To overcome this problem, we have proposed a semivectorial horizontally wide-angle BPM (HWA-BPM) based on the ADI scheme, in which the (1,1) Padé approximant is applied to only the horizontal direction, and the second-order FD formula (IFD2) is used to approximate the spatial second derivatives [13]. The HWA formulation reduces the splitting error to the first order, even though the noniterative ADI procedure is utilized. Very recently, the 3-D scalar WA-BPM with the ADI scheme was developed [14]. Although not explicitly described in [14], our careful examination showed that the splitting error still remains the zeroth order.

This letter is devoted to the development of a highly-accurate 3-D semivectorial HWA-BPM. In the formulation, the higher order Padé approximants are successfully incorporated into the horizontal direction with the help of the multistep method, and the IFD4 is utilized to approximate the spatial second derivatives together with the ADI scheme, while maintaining the tridiagonal matrices. As in the (1,1) Padé approximant [13], the splitting error is reduced to the first order. Numerical results for a tilted step-index waveguide demonstrate the effectiveness of the multistep HWA-BPM. Also shown is the application to the analysis of a multimode interference (MMI) coupler.

## II. Formulation

The equation of the 3-D HWA-BPM for an $(N,N)$ Padé approximant operator is expressed as

$$\left[1+\sum_{m=1}^{N} a_m(D_{xx}+\nu)^m+\frac{j\Delta z}{4kn_0}D_{yy}\right]\phi^{l+1} = \left[1+\sum_{m=1}^{N} a_m^*(D_{xx}+\nu)^m-\frac{j\Delta z}{4kn_0}D_{yy}\right]\phi^{l} \quad (1)$$

in which $*$ denotes the complex conjugate, and the Padé approximant is applied to only the $x$ direction, while keeping the paraxial approximation in the $y$ direction (the equation for $N=1$ corresponds to (3) in [13]). In (1), the definitions of $\phi$, $D_{xx}$, $D_{yy}$, and $\nu$ appear in [13], and $k$ and $n_0$ represent the free-space wavenumber and the reference refractive index to be appropriately chosen, respectively. The coefficients $a_m$'s are readily determined by the basic equation of the $(N,N)$ Padé approximant for a 2-D problem [3].

To solve (1) with the ADI scheme, we split it as follows:

$$\left[1+\sum_{m=1}^{N} a_m(D_{xx}+\nu)^m\right]\left[1+\frac{j\Delta z}{4kn_0}D_{yy}\right]\phi^{l+1} = \left[1+\sum_{m=1}^{N} a_m^*(D_{xx}+\nu)^m\right]\left[1-\frac{j\Delta z}{4kn_0}D_{yy}\right]\phi^{l}. \quad (2)$$

Manuscript received June 19, 2006; revised August 23, 2006. This work was supported in part by the "University-Industry Joint Research" Project for Private Universities: matching fund subsidy from MEXT, 2003–2007.

The authors are with the Faculty of Engineering, Hosei University, Tokyo 184-8584, Japan (e-mail: shiba@k.hosei.ac.jp).

Digital Object Identifier 10.1109/LPT.2006.887201

Furthermore, we factor the first brackets of both sides of (2) into a series of simpler Padé (1,1) operators [4]

$$\begin{aligned}&[1+b_1(D_{xx}+\nu)]\,[1+b_2(D_{xx}+\nu)]\cdots\\&\quad[1+b_N(D_{xx}+\nu)]\left[1+\frac{j\Delta z}{4kn_0}D_{yy}\right]\phi^{l+1}\\&\quad=[1+b_1^*(D_{xx}+\nu)]\,[1+b_2^*(D_{xx}+\nu)]\cdots\\&\quad[1+b_N^*(D_{xx}+\nu)]\left[1-\frac{j\Delta z}{4kn_0}D_{yy}\right]\phi^{l}.\end{aligned}\tag{3}$$

The coefficients $b_m$'s can be determined by the one-time solution of an $N$th-order complex algebraic equation. Here, we approximate $D_{\alpha\alpha}$, in which $\alpha$ represents $x$ or $y$, using the IFD4, i.e., $D_{\alpha\alpha}=\bar{D}_{\alpha\alpha}/\tilde{D}_{\alpha\alpha}$. The definitions of the three point FD operators $\bar{D}_{\alpha\alpha}$ and $\tilde{D}_{\alpha\alpha}$ are found in [7].

Introducing the intermediate field $\phi^{l+1/2}$, we derive the following ADI algorithm of the multistep HWA-BPM with the $(N,N)$ Padé approximant:

$$\begin{aligned}&\left[\tilde{D}_{yy}+\frac{j\Delta z}{4kn_0}\bar{D}_{yy}\right]\phi^{l+1/2}\\&\quad=\left[(1+b_1^*\nu)\,\tilde{D}_{xx}+b_1^*\bar{D}_{xx}\right]\times\left[(1+b_2^*\nu)\,\tilde{D}_{xx}+b_2^*\bar{D}_{xx}\right]\cdots\\&\qquad\left[(1+b_N^*\nu)\,\tilde{D}_{xx}+b_N^*\bar{D}_{xx}\right]\phi^{l}\end{aligned}\tag{4}$$

$$\begin{aligned}&\left[(1+b_1\nu)\tilde{D}_{xx}+b_1\bar{D}_{xx}\right]\left[(1+b_2\nu)\tilde{D}_{xx}+b_2\bar{D}_{xx}\right]\cdots\\&\left[(1+b_N\nu)\tilde{D}_{xx}+b_N\bar{D}_{xx}\right]\phi^{l+1}\\&\quad=\left[\tilde{D}_{yy}-\frac{j\Delta z}{4kn_0}\bar{D}_{yy}\right]\phi^{l+1/2}.\end{aligned}\tag{5}$$

First, we obtain $\phi^{l+1/2}$ in (4) by the solution of a tridiagonal system of linear equations. To calculate $\phi^{l+1}$, we next decompose (5) into an $N$-step algorithm [4]. It is noteworthy that each step maintains a tridiagonal form, which can be efficiently solved by the Thomas algorithm. As a result, the HWA procedure proposed here requires the solutions of $1+N$ tridiagonal sets of linear equations. It is worth mentioning that the splitting error of the present HWA-BPM is reduced to the first-order as in the (1,1) Padé case [13], which is readily confirmed by expanding (3).

## III. Numerical Results

We investigate the effectiveness of the multistep HWA-BPM through the analyses of a tilted waveguide and an MMI coupler. In this letter, we study up to the (2,2) approximant, since approximants higher than (2,2) are not necessary required to generate reasonable results in the following waveguide analyses. The perfectly matched layer absorbing boundary condition [15] is used for each numerical example.

First, we analyze a tilted step-index waveguide, which is the same as that used in [13]. The tilt angle is set at $\theta=30^\circ$, $40^\circ$, or $45^\circ$. The sampling widths are taken to be $\Delta x=a/(N_x\cos 45^\circ)\simeq\Delta y=0.1$ $\mu$m and $\Delta z=\Delta x$, in which the core width is $a=5$ $\mu$m and the number of sampling points in the core along the $x$ direction is $N_x=70$. It is noted that for $\theta=45^\circ$ all the interfaces between the core and cladding lie midway between the sampling points. In contrast, for $\theta=30^\circ$ and $40^\circ$ the waveguide is discretized with the so-called staircase approximation.

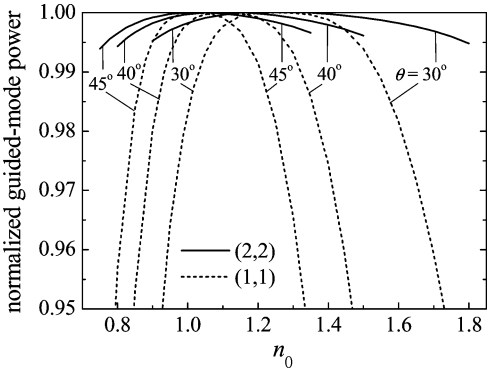


Fig. 1. Normalized guided-mode power as a function of $n_0$. Each data is obtained using the same sampling widths $\Delta x\simeq\Delta y=0.1$ $\mu$m and $\Delta z=\Delta x$ with the IFD4.

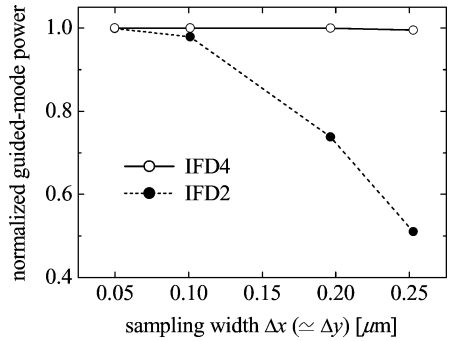


Fig. 2. Normalized guided-mode power as a function of transverse sampling width $\Delta x(\simeq\Delta y)$ with $\Delta z=\Delta x$. Each data is obtained with the Padé (2,2) approximant. The tilt angle is set at $\theta=45^\circ$ and $n_0$ is chosen to be $n_{\rm eff}\cos 45^\circ$.

Fig. 1 shows the guided-mode power of the $E_y$ field (the quasi-TM mode) observed at $z=40$ $\mu$m, normalized to the input power of the fundamental eigenmode, as a function of reference refractive index $n_0$. When the eigenmode field propagates without deformation, the normalized guided-mode power remains unity. It is clear that the increase in the Padé order leads to the improvement in accuracy for each tilt angle. This also means that the phase error of the propagating field is successfully suppressed regardless of the choice of $n_0$ [5]. In addition, the normalized guided-mode power becomes insensitive to the choice of $n_0$ with a decrease in the tilt angle. For each tilt angle, the maximum guided-mode power is observed around $n_0=n_{\rm eff}\cos\theta$, in which $n_{\rm eff}$ is the effective index of the guided mode.

Note that the computation time of the IFD4-based method does not significantly increase when compared with the IFD2 counterpart for specific sampling widths, since the computation efforts are virtually the same for both methods due to the three-point FD formulas (e.g., the computation time using a PC with a 3.4-GHz CPU is about 165 s for the IFD4, and 123 s for the IFD2 with $\Delta x\simeq\Delta y=0.2$ $\mu$m). Nevertheless, the improved accuracy for the IFD4 is remarkable as shown in Fig. 2, where the guided-mode power at $z=40$ $\mu$m as a function of $\Delta x(\simeq\Delta y)$ is presented. To obtain a converged solution, the IFD4 requires $\Delta x\simeq\Delta y=0.2$ $\mu$m, while the IFD2 $\Delta x\simeq\Delta y=0.05$ $\mu$m. This means that $\Delta x$ and $\Delta y$ for the IFD4 are

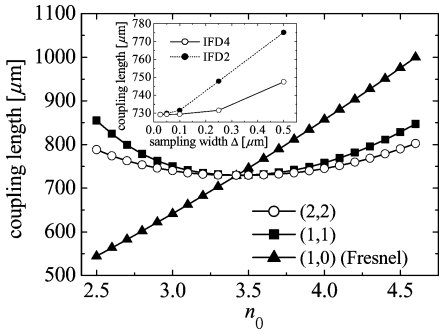


Fig. 3. Coupling length versus $n_0$ using the IFD4. The sampling widths are $\Delta x = \Delta y \equiv \Delta = 0.1\ \mu$m and $\Delta z = \Delta$. The inset shows the convergence behavior of the coupling length with respect to $\Delta$ using the (2,2) approximant, in which $\Delta z$ is fixed to be 0.1 $\mu$m and $n_0$ is chosen to be 3.42.

chosen to be four times as large as those for the IFD2. Therefore, the total number of sampling points for the IFD4 is reduced to one sixteenth of that of the IFD2, demonstrating a significant reduction in the computation time.

It should be noted that even when a straight waveguide is treated, the use of the Fresnel-based BPM gives rise to the phase error unless $n_0$ is chosen to be close to $n_{\text{eff}}$. For an MMI coupler, there exist several guided modes with their own $n_{\text{eff}}$'s, which determine the coupler length of the MMI section. These facts indicate that the phase error of the Fresnel-based BPM may affect the accuracy in calculating the coupler length. In contrast, the phase error is significantly reduced when the WA-BPM is utilized. Therefore, we next investigate how the HWA-BPM offers reasonable accuracy in calculating the coupler length of a rib MMI waveguide, even when $n_0$ is varied.

The cross section of the input waveguide connected to the MMI coupler is the same as that of Fig. 1 in [10]. The width of the MMI section (15 $\mu$m) is five times as wide as that of the input waveguide. The wavelength is $\lambda = 1.15\ \mu$m. The sampling widths are $\Delta x = \Delta y \equiv \Delta = \Delta z = 0.1\ \mu$m. Fig. 3 depicts the coupling length of the quasi-TM mode in the MMI section versus $n_0$, at which the overlap integral between the input and propagating fields becomes the first maximum. As can clearly be seen in Fig. 3, the use of the (2,2) approximant significantly suppresses the dependence of $n_0$ on the coupling length. On the contrary, the results obtained from the Fresnel-based BPM depend on the choice of $n_0$. Consequently, the HWA-BPM is effective not only for the wide-angle analysis, but also for the paraxial analysis involving several guided modes such as MMI couplers.

The inset of Fig. 3 displays the convergence behavior of the coupling length with respect to $\Delta$ using the (2,2) approximant. It is seen that, when compared with the IFD2, the IFD4 provides faster convergence in which the difference in the coupling length is kept within about 0.2 $\mu$m for $\Delta \leq 0.1\ \mu$m.

As discussed above, the present method offers the wide-angle feature in the $x$ direction, while assuming the paraxial approximation in the $y$ direction. Therefore, strictly speaking, the wave to be treated must be paraxial in the $y$ direction. It can be expected, however, that the accuracy with respect to the $y$ direction is maintained provided that $n_0$ is chosen to be an (averaged) effective index of the beam propagating toward a specific $y$ direction, while the wide-angle feature in the $x$ direction is retained to some extent.

## IV. Conclusion

We have developed a multistep HWA-BPM based on the GD scheme. The fourth-order accurate FD formula (IFD4) allows us to employ large spatial sampling widths when compared with the second-order counterpart (IFD2), leading to efficient calculations. Through the analyses of the tilted waveguide and the MMI coupler, it is demonstrated that the present HWA formulation offers high accuracy over a wide range of reference refractive index.

## References

[1] D. Yevick and M. Glasner, "Analysis of forward wide-angle light propagation in semiconductor rib waveguides and integrated-optic structures," *Electron. Lett.*, vol. 25, no. 23, pp. 1611–1613, Nov. 1989.

[2] ——, "Forward wide-angle light propagation in semiconductor rib waveguides," *Opt. Lett.*, vol. 15, no. 3, pp. 174–176, Feb. 1990.

[3] G. R. Hadley, "Wide-angle beam propagation using Padé approximant operators," *Opt. Lett.*, vol. 17, no. 20, pp. 1426–1428, Oct. 1992.

[4] ——, "Multistep method for wide-angle beam propagation," *Opt. Lett.*, vol. 17, no. 24, pp. 1743–1745, Dec. 1992.

[5] J. Yamauchi, J. Shibayama, M. Sekiguchi, and H. Nakano, "Improved multistep method for wide-angle beam propagation," *IEEE Photon. Technol. Lett.*, vol. 8, no. 10, pp. 1361–1363, Oct. 1996.

[6] J. Shibayama, K. Matsubara, M. Sekiguchi, J. Yamauchi, and H. Nakano, "Efficient nonuniform schemes for paraxial and wide-angle finite-difference beam propagation methods," *J. Lightw. Technol.*, vol. 17, no. 4, pp. 677–683, Apr. 1999.

[7] Y. P. Chiou, Y. C. Chiang, and H. C. Chang, "Improved three-point formulas considering the interface conditions in the finite-difference analysis of step-index optical devices," *J. Lightw. Technol.*, vol. 18, no. 2, pp. 243–251, Feb. 2000.

[8] J. Yamauchi, M. Koshihara, and H. Nakano, "Numerical analysis of a waveguide-based demultiplexer with two multiple-layer filters," *IEEE Photon. Technol. Lett.*, vol. 17, no. 2, pp. 366–368, Feb. 2005.

[9] H. Zhang, N. N. Feng, and W. P. Huang, "Wide-angle beam propagation method based on high-accuracy finite-difference formulas," presented at the Integr. Photon. Res. Appl., Uncasville, CT, Apr. 2006, ITuA2.

[10] J. Yamauchi, T. Murata, and H. Nakano, "Semivectorial H-field analysis of rib waveguides by a modified beam-propagation method based on the generalized Douglas scheme," *Opt. Lett.*, vol. 25, no. 24, pp. 1771–1773, Dec. 2000.

[11] D. Yevick, J. Yu, W. Bardyszewski, and M. Glasner, "Stability issues in vector electric field propagation," *IEEE Photon. Technol. Lett.*, vol. 7, no. 6, pp. 658–660, Jun. 1995.

[12] S. L. Chui and Y. Y. Lu, "Wide-angle full-vector beam propagation method based on an alternating direction implicit preconditioner," *J. Opt. Soc. Amer. A*, vol. 21, no. 3, pp. 420–425, Mar. 2004.

[13] J. Shibayama, T. Takahashi, J. Yamauchi, and H. Nakano, "A three-dimensional horizontally wide-angle noniterative beam-propagation method based on the alternating-direction implicit scheme," *IEEE Photon. Technol. Lett.*, vol. 18, no. 5, pp. 661–663, Mar. 2006.

[14] C. Ma and E. V. Keuren, "A simple three dimensional wide-angle beam propagation method," *Opt. Express*, vol. 14, no. 11, pp. 4668–4674, May 2006.

[15] W. P. Huang, C. L. Xu, W. Lui, and K. Yokoyama, "The perfectly matched layer (PML) boundary condition for the beam propagation method," *IEEE Photon. Technol. Lett.*, vol. 8, no. 5, pp. 649–651, May 1996.